Search for Heavy Neutral Leptons with IceCube DeepCore

Dissertation
zur Erlangung des akademischen Grades
doctor rerum naturalium
(Dr. rer. nat.)

im Fach: Physik
Spezialisierung: Experimentalphysik

eingereicht an der
Mathematisch-Naturwissenschaftlichen Fakultät
der Humboldt-Universität zu Berlin

von
Leander Fischer M. Sc.
geboren am 24. Oktober 1992
in Heidelberg

Präsidentin der Humboldt-Universität zu Berlin
Prof. Dr. Julia von Blumenthal

Dekanin der Mathematisch-Naturwissenschaftlichen Fakultät
Prof. Dr. Caren Tischendorf

Zusammenfassung

Zusammenfassung . . .

Abstract

Abstract . . .
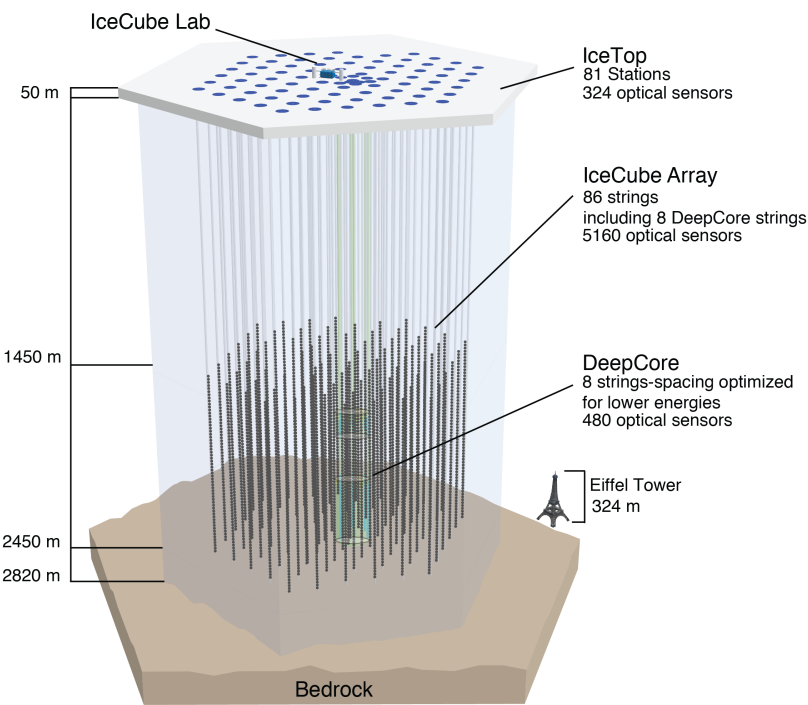
Todo list

Contents

List of Figures

List of Tables

The IceCube Neutrino Observatory

The IceCube Neutrino Observatory [1] is a cubic-kilometer, ice-Cherenkov detector located at the geographic South Pole. IceCube utilizes the Antarctic glacial ice as detector medium to observe neutrinos by measuring the Cherenkov light produced from secondary charged particles with optical modules. It was deployed between 2006 and 2011 and has been taking data since the installation of the first modules. The primary goal of IceCube is the observation of astrophysical neutrinos as a telescope, but it can also be used to study fundamental particle physics properties by measuring atmospheric neutrinos as well as studying cosmic rays.

This chapter first describes the main- and sub-array of the detector and its detection module in Section 1.1, the propagation of particles through ice is explained in Section 1.2, and finally, the signatures that IceCube can observer of the different particles are introduced in Section 1.3.

[1]: Aartsen et al. (2017), "The IceCube Neutrino Observatory: instrumentation and online systems"

1.1 IceCube Detector Components

Figure 1.1: Overview of the IceCube detector showing the in-ice main- and sub-array IceCube and DeepCore, IceTop, and the IceCube Lab. From [1].

The full IceCube detector array consists of 86 vertical, in-ice strings and 81 surface stations as shown in Figure 1.1. The in-ice part is composed of 60 optical modules per string deployed at depths of 1450 m-2450 m below the ice, while the surface stations of the comic air-shower array, *IceTop*, are ice-filled tanks. The surface stations and the majority of the strings are arranged in a hexagonal grid with the operations building, the *IceCube Laboratory* (ICL), central to the grid on the surface. A top view of the hexagonal arrangement is shown in Figure 1.4. The in-ice

array is designed to detect neutrinos in the energy range from $\mathcal{O}(\text{GeV})$ to $\mathcal{O}(\text{PeV})$.

1.1.1 Digital Optical Modules and the Antarctic Ice

[2]: Price et al. (2000), "Age vs depth of glacial ice at South Pole"

The IceCube detection medium is the Antarctic glacial ice, which was formed over 100 000 years by accumulation of snow that was subsequently compressed by its own weight to form a dense crystal structure [2]. As a result of this formation process, the optical properties, scattering and absorption, primarily change with depth. Within the detector volume the absorption length ranges from 100 m-400 m, while the scattering length lies between 20 m-100 m. They are correlated, with the absorption length being roughly four times the scattering length [3]. The vertical distribution of scattering and absorption length can be seen in Figure 1.2, where one dominant feature is the *dust layer* between 2000 m to 2100 m depth. This region has a higher concentration of dust particles that where deposited in a period of high volcanic activity, which leads to bad optical properties in form of larger scattering and absorption.

[3]: Abbasi et al. (2022), "In-situ estimation of ice crystal properties at the South Pole using LED calibration data from the IceCube Neutrino Observatory"
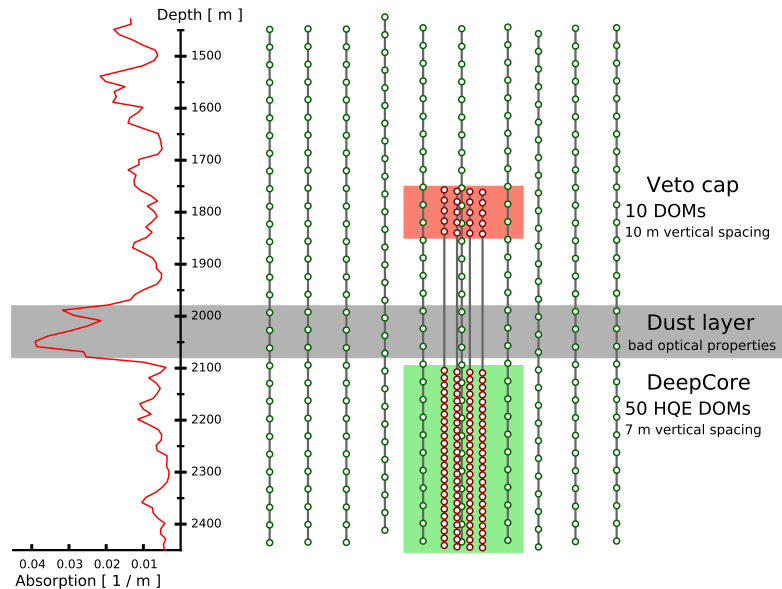
Figure 1.2: xx

exchange for figure with scattering (check abs/sca is cocrrect)

mention/cite dust logger paper/procedure?

[4]: Abbasi et al. (2009), "The IceCube data acquisition system: Signal capture, digitization, and timestamping"

The ice is instrumented by 5160 optical sensors called Digital Optical Modules (DOMs) [4], which can detect the Cherenkov light produced by charged particles traveling through the ice. Each DOM is made of a spherical glass housing, containing a downward-facing Photomultiplier Tube (PMT), the main board with control, readout, and processing-electronics, and a LED flasher board for calibration purposes. The design and the individual components of a DOM can be seen in Figure 1.3.

The majority of PMTs are the 10 ″ Hamamatsu R7081-02, which have a bialkali photocathode and are sensitive to wavelengths in the range of 300 nm to 650 nm, with a peak quantum efficiency (quantum efficiency of 25% at 390 nm. In the central part of the IceCube array the peak efficiency reaches 34%. The dark count rate in the temperature range of −40 °C to −20 °C is ~300 Hz. The DOM electronics measure the PMT voltage and control the gain. At a voltage crossing of the equivalent to 0.25 PE the waveform readout is activated [4]. Only when either one of the nearest

[4]: Abbasi et al. (2009), "The IceCube data acquisition system: Signal capture, digitization, and timestamping"

or next to nearest DOMs above or below also saw a voltage crossing within a 1 μs time window [1], the voltages are digitized and send to the ICL. Through the application of a waveform unfolding algorithm, called *WaveDeform* [5], the waveforms are compressed and the results are the reconstructed times and charges of the photo-electrons. This is the basis for all further IceCube data processing.

The PMT is covered with a mu-metal grid (made from wire mesh), shielding the photocathode from Earth's magnetic field and it is optically coupled to the glass sphere by RTV silicone gel. The glass sphere is a pressure vessel, designed to withstand both the constant ice pressure and the temporary pressure during the refreezing process of the water in the drill hole during deployment (peaking at around 690 bar). The sphere is held by a harness that connects the DOMs along a string and also guides the cable beside them.

The flasher board controls 12 LEDs that produce optical pulses in bright UV. The LEDs can be pulsed separately or in combination with variable output levels and pulse lengths. Using the known information of the light source positions and times this can be used for in-situ calibration of the detector by measuring absorption and scattering properties of the ice. Calibrating the optical efficiency of the DOMs itself is more accurately done using minimum ionizing muons [6], since the total amplitude of the LED light is not well known.

1.1.2 IceCube

The 78 strings that are arranged in a hexagonal pattern from the main part of the in-ice array, which is called *IceCube*. With a ~125 m horizontal spacing between the strings and a ~17 m vertical spacing between DOMs, IceCube has a lower energy threshold of around 100 GeV. IceCube was designed to detect astrophysical neutrinos with energies above 1 TeV.

The coordinate system that is used in IceCube is centered at 46500'E, 52200'N at an elevation of 883.9 m [1]. Per definition, it's a right-handed coordinate system where the y-axis points along the Prime Meridian (Grid North) towards Greenwich, UK, and the x-axis points 90° clockwise from the y-axis (Grid East). The z-axis is normal to the ice surface, pointing upwards. For IceCube analyses depth is defined as the distance along the z axis from the ice surface, assumed to be at an elevation of 2832 m.

1.1.3 DeepCore

The additional 8 strings form a denser sub-array of IceCube called *DeepCore* [7]. It's located at the bottom-center of the in-ice array and its *fiducial volume* also includes the 7 surrounding IceCube strings as shown in Figure 1.4. The strings in this region have a closer average horizontal distance of about 70 m. Th lower 50 DeepCore DOMs on each string are placed in the region of clear ice below the dust layer between 2100 m to 2450 m depth, where their vertical spacing is ~7 m. The remaining 10 modules on each string are placed above the dust layer to be used as veto against atmospheric muons. Additionally, the DeepCore DOMs

1: This is referred to as a *hard local coincidence (HLC)*.

[5]: Aartsen et al. (2014), "Energy Reconstruction Methods in the IceCube Neutrino Telescope"
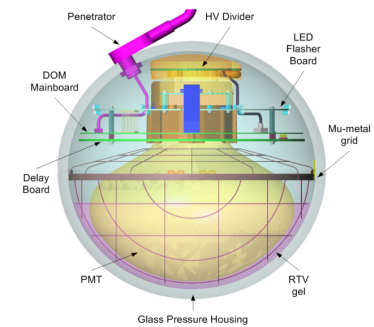

Figure 1.3: Design and components of a Digital Optical Module (DOM) [4]

[6]: Kulacz (2019), "In Situ Measurement of the IceCube DOM Efficiency Factor Using Atmospheric Minimum Ionizing Muons"

[1]: Aartsen et al. (2017), "The IceCube Neutrino Observatory: instrumentation and online systems"

[7]: Abbasi et al. (2012), "The design and performance of IceCube DeepCore"
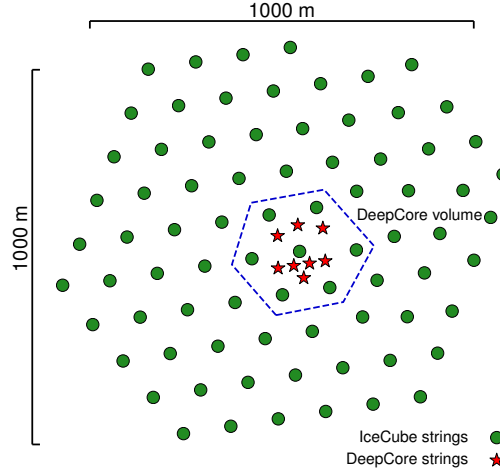
Figure 1.4: Top view of the IceCube array.

are equipped with higher quantum efficiency PMTs. The combination of the denser spacing and the high quantum efficiency modules, leads to a lower energy detection threshold of around 5 GeV, allowing the observation of atmospheric neutrinos, which are mostly in the energy range of 10 GeV to 100 GeV. The main analysis performed with DeepCore is an atmospheric neutrino oscillation measurement, but the large flux of atmospheric neutrinos allows for many other Beyond Standard Model searches, such as searches for dark matter, non-standard interactions, or sterile neutrinos.

> (Re-)write introduction for PhD thesis (just copy paste from M.Sc.). (everything below)

1.2 Propagation of Particles in Ice

When charged particles travel through matter they interact and lose energy by several interaction processes. The Cherenkov light emitted by the particles as described in Section Section 1.2.1 only contributes a small amount to the total energy loss. The dominant processes depend on the type of Cherenkov light source, which we can broadly categorize into the three groups: quasi-continuous energy loss by muons, electromagnetic cascades, and hadronic cascades.

Muons   lose their energy mainly by *ionization*, *bremsstrahlung*, *pair production* and the *photo-nuclear interaction*. Considering that ionization only has a weak energy dependence for muons above 1 GeV and combining the other three components into one, the total energy loss is given by

$$-\frac{\mathrm{d}E}{\mathrm{d}x} = a_I(E) + b_R(E) \cdot E, \tag{1.1}$$

where E is the energy and $a_I(E)$ and $b_R(E) \cdot E$ are the energy loss by ionization and the combined radiative losses, respectively. For the energy range of interest for this work, the parameters $a_I(E)$ and $b_R(E)$ only have a weak energy dependence and equation Equation 1.1 reduces to

$$-\frac{\mathrm{d}E}{\mathrm{d}x} = a + b \cdot E. \tag{1.2}$$

This description results in a critical energy $E_{crit} = a/b$ separating the two energy regimes where ionization or radiative losses are dominant. Typical values are $a \approx 2.59\,\text{MeV/cm}$ and $b \approx 3.63 \cdot 10^{-6}\,\text{cm}^{-1}$ [8] leading to a critical energy of $\sim 770\,\text{GeV}$. Since the considered energy range for atmospheric neutrino oscillations is below the critical energy we only consider ionization losses by setting $b = 0$ which easily relates the range of a muon R_μ to its initial energy by

[8]: Chirkin et al. (2004), "Propagating leptons through matter with Muon Monte Carlo (MMC)"

$$R = \frac{E_0}{a}. \tag{1.3}$$

With equation Equation 1.3 it is clear that by measuring the length of a muon track, its energy can be estimated if the full track is contained in IceCube. This treatment is only an approximation and does not take into account the stochastic nature of some of the energy losses. Especially bremsstrahlung and photo-nuclear interactions occur rarely, but when they happen, they deposit a large amount of energy. More detailed information is found in [9].

[9]: Raedel (2012), "Simulation Studies of the Cherenkov Light Yield from Relativistic Particles in High-Energy Neutrino Telescopes with Geant4"

1.2.1 Cherenkov Effect

[10]: Cherenkov (1937), "Visible Radiation Produced by Electrons Moving in a Medium with Velocities Exceeding that of Light"

Cherenkov radiation is emitted when a charged particle moves through a medium with a velocity that is greater than the speed of light in that medium. The continuous energy loss due to the emission of Cherenkov radiation is small, at the order of $\mathbb{O}(10^{-4})$, as compared to the main energy losses that will be described in Section Section 1.2.2. The observation of this radiation in IceCube and DeepCore, however, is fundamental for the detection of the charged particles originating from the neutrino interactions that were outlined in Section Section **??**. The Cherenkov effect was first observed by Pavel Cherenkov in 1934 [10]. As can be derived from trigonometry, the Cherenkov light is emitted in a parallel wavefront at the Cherenkov angle

[11]: Euler (2014), "Observation of oscillations of atmospheric neutrinos with the IceCube Neutrino Observatory"

[12]: Frank et al. (1937), "Coherent visible radiation from fast electrons passing through matter"

$$\theta_c = \arccos\left(\frac{1}{\beta n}\right), \tag{1.4}$$

[13]: Rädel et al. (2012), "Calculation of the Cherenkov light yield from low energetic secondary particles accompanying high-energy muons in ice and water with Geant4 simulations"

with n being the refractive index of the medium and β the speed of the particle in units of the speed of light. A sketch of the wavefront is shown in Figure Figure 1.5, where the black circles depict spherically emitted light and the blue line is the formed Cherenkov light front. Typical values for the Antarctic ice are $n \approx 1.3$ and as a result $\theta_c \approx 41°$ [11]. Additionally, one can calculate the number of photons produced by a Cherenkov emitter based on the description in [12]. For a wavelength λ with ($300\,\text{nm} < \lambda < 500\,\text{nm}$) 250 photons per cm are emitted assuming a very relativistic particle with $\beta \simeq 1$ [13].
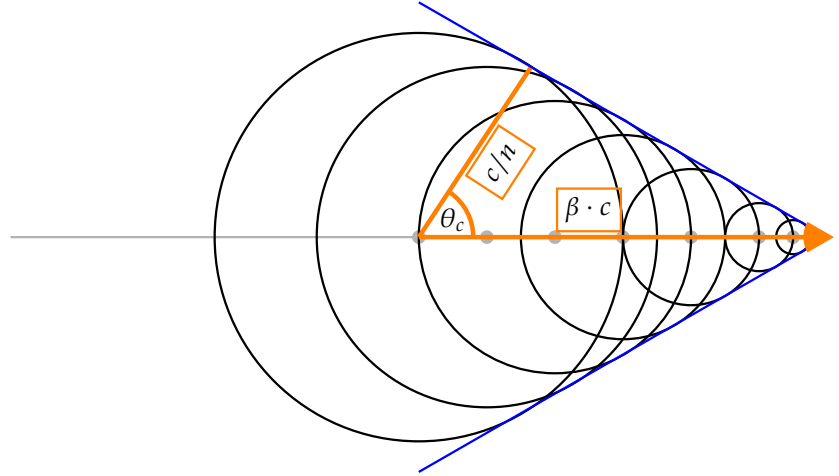
Figure 1.5: Schematic formation of the Cherenkov light front (blue) produced by a charged particle traveling faster than the speed of light in the medium. The black circles are spherically emitted light and the orange arrow shows the direction of the particle.

1.2.2 Energy Losses

Muons

Electromagnetic Showers

Electromagnetic cascades are induced by electrons and positrons or photons. All of them are either produced directly in the neutrino interactions or in interactions of secondary particles. Photons lose energy via pair production whereas for electrons and positrons the dominant energy loss is due to bremsstrahlung. For both cases, the interaction process happens repeatedly and an electromagnetic shower is formed when pair production and bremsstrahlung take place in turn. Every time one of the interactions takes place, more electrons and positrons or photons are produced with smaller energy. This proceeds until the energy of the particles falls below the critical energy E_c and the remaining energy is quickly lost. For electrons and positrons, this happens through ionization and excitation of the surrounding atoms. For photons, the Compton effect and the photoelectric effect become the dominant energy losses. Electromagnetic showers are characterized by the radiation length X_0 at which the energy of electrons or positrons is reduced to $1/e$ of their initial energy. For photons, X_0 is 7/9 of the mean free path for pair production. For ice, the critical energy is $E_c \approx 78\,\text{MeV}$ and the radiation length is $X_0 \approx 39.3\,\text{cm}$ [14].

[14]: Tanabashi et al. (2018), "Review of Particle Physics"

Hadronic Showers

Hadronic cascades are always produced in the neutrino interactions described in Section Section **??**, either from the breaking nucleus or as decay products. Similar to an electromagnetic cascade, a hadronic cascade forms as a result of the production of secondary particles from the strong interactions of hadrons with the traversed matter. Hadronic cascades also contain an electromagnetic component, for example through the decay of neutral pions into two photons. The shower profile and the light emission are very dependent on the produced particle type, which leads to larger fluctuations between individual showers with the same energy. The observed energy also varies, because energy gets lost in the hadronic

binding process and muons and neutral particles produce less light and no light, respectively. On top of that, hadrons have a higher energy threshold for Cherenkov light production, due to their higher mass. The relative brightness of hadronic showers as compared to electromagnetic showers is given by [9]

$$F(E) = \frac{T_{\text{hadron}}}{T_{\text{EM}}}, \tag{1.5}$$

where $T_{\text{hadron/EM}}$ is the total track length of a hadronic/electromagnetic shower with the same energy. The ratio $F(E)$ is always smaller than 1, but increases with energy as the electromagnetic fraction of the hadronic cascade becomes larger. A more detailed parameterization of $F(E)$, as well as fitted values for several particle types, can be found in [9].

[9]: Raedel (2012), "Simulation Studies of the Cherenkov Light Yield from Relativistic Particles in High-Energy Neutrino Telescopes with Geant4"

[9]: Raedel (2012), "Simulation Studies of the Cherenkov Light Yield from Relativistic Particles in High-Energy Neutrino Telescopes with Geant4"

1.3 Particle Signatures in IceCube

1.3.1 Neutrinos

1.3.2 Atmospheric muons

Standard Model Background Simulation and Data Processing | 2

2.1 Event Generation

2.1.1 Neutrinos

2.1.2 Muons

2.2 Detector Simulation

2.2.1 Photon Propagation

2.2.2 Detector Respones

2.3 Processing

2.3.1 Trigger and Online Filter

2.3.2 Offline Filter

2.3.3 Hit Selection

To select hits that originated from direct photons, a procedure closely related to the one described in [15] is applied. The cleaning is based on removing hits from DOMs that could have originated from light emitted by any of the other hit DOMs on the same string. The selection solely uses the time of arrival (TOA) of the pulses. It is carried out for every detected event in the following steps:

[15]: Garza (2014), "Measurement of neutrino oscillations in atmospheric neutrinos with the IceCube DeepCore detector"

  (i) Select strings where at least 3 DOMs have seen light.
 (ii) Every hit DOM is characterized by the time of the earliest pulse (above a threshold of 0.1 photoelectron (PE)) and the integrated charge of all pulses.
(iii) For every string passing these criteria the following steps are performed:

   (a) Remove DOMs with hit outside of a time window of [-250 ns, +2000 ns] around the median TOA of all hits on the string.
   (b) Using the DOM with the highest charge as reference (estimate for point of closest approach), check if any of the other DOMs on the string lies in the time window

$$\left[t_r - \frac{d_{r,i}}{c_{\text{ice}}} - t_{\text{delay}}, t_r + \frac{d_{r,i}}{c_{\text{ice}}} + t_{\text{delay}} \right], \qquad (2.1)$$

where t_r is the TOA of the reference DOM, $d_{r,i}$ is the absolute distance between the two DOMs considered, c_{ice} is the speed of light in ice and t_{delay} is the allowed time delay. A time delay

of 20 ns is used to limit the selection to photons with little scattering.

(c) For each of the selected DOMs, it is now verified that, compared to each of the other selected DOMs, none was hit after the time t_{max}

$$t_{max} = t_i + \frac{d_{i,j}}{c_{ice}} + t_{delay},\qquad(2.2)$$

where the subscripts i and j stand for the two DOMs in questions, and all combinations are checked.

(d) As the last step, it is checked whether there are more than six empty modules between selected modules. Keeping the DOM with the largest charge, the other DOMs are checked going upwards and downwards along the string. Finally, only strings that still have three or more selected DOMs are kept and their hits are identified as direct pulses.

2.3.4 Reconstruction

There are several methods to select and reconstruct events in IceCube. At energies around 10-40 GeV, where we expect the oscillation signal, the events are faint and only a few DOMs detect light. One approach for the reconstruction of such events is described in this section. The reconstruction uses only photons that traveled along a straight line - called *direct* photons. Using direct photons has the benefit of reducing the systematic biases caused by the large variations of the bulk ice properties; scattering and absorption. With an average distance of 70 m between strings in DeepCore and an effective scattering length of about 50 m [16], there will always be a fraction of direct photons arriving at the DOMs. The used method applies a stepwise procedure, where first a cleaning routine selects events with direct photons as described in Section Section 2.3.3. Afterward, the direction of the particle is reconstructed and finally the energy is determined as outlined in Sections Section 2.3.4.

[16]: Lundberg et al. (2007), "Light tracking for glaciers and oceans: Scattering and absorption in heterogeneous media with Photonics"

FLERCNN Event Reconstruction and Classification

Didn't copy over SANTA/LEERA since I need the FLERCNN desciption here.

Standard Model Event Topologies

The signals that IceCube detects vary depending on the neutrino flavor and interaction type of the event. The two main signatures that can be observed are track-like and cascade-like events. The observed Cherenkov light is produced by the secondary particles originating from the neutrino interactions described in Section Section **??**. Table Table **??** shows an overview of the possible event signatures. Minimum ionizing muons can travel for long distances and are seen as extended light signatures called tracks. Muons can come from ν_μ-CC interactions or from ν_τ-CC followed by the decay of the τ to a muon. However, the τ only decays to a muon with a branching ratio of BR=17 %.

Cascades are the light signal produced by the EM/hadronic showers described in Section Section 1.2.2. They come from ν_e-CC and most of the ν_τ-CC interactions because the electron and the tau lose all their energy quickly and only travel a short distance. They are also produced in all ν-NC interactions since only the hadronic shower is observable and the produced neutrino escapes unseen. The cascades at the energies considered in this work have a smaller radius than the spacing of the DOMs and are therefore seen as point-like light emitters.

The existence of the two types of event topologies and their origins imply that by identifying track-like events we can identify events coming (mainly) from ν_μ-CC interactions and therefore obtain a flavor identification. This is a crucial part of performing an oscillation analysis as will be further discussed in Section Section **??**.

2.4 Systematic Uncertainties

2.4.1 Detector Property Variations

2.4.2 Atmospheric Flux

APPENDIX

A

First Appendix

Bibliography

Here are the references in citation order.

[1]   M. G. Aartsen et al. "The IceCube Neutrino Observatory: instrumentation and online systems". In: *Journal of Instrumentation* 12.3 (Mar. 2017), P03012. DOI: 10.1088/1748-0221/12/03/P03012 (cited on pages 1, 3).

[2]   P. B. Price, K. Woschnagg, and D. Chirkin. "Age vs depth of glacial ice at South Pole". In: *Geophysical Research Letters* 27.14 (2000), pp. 2129–2132. DOI: https://doi.org/10.1029/2000GL011351 (cited on page 2).

[3]   R. Abbasi et al. "In-situ estimation of ice crystal properties at the South Pole using LED calibration data from the IceCube Neutrino Observatory". In: *The Cryosphere Discussions* 2022 (2022), pp. 1–48. DOI: 10.5194/tc-2022-174 (cited on page 2).

[4]   R. Abbasi et al. "The IceCube data acquisition system: Signal capture, digitization, and timestamping". In: *Nuclear Instruments and Methods in Physics Research Section A: Accelerators, Spectrometers, Detectors and Associated Equipment* 601.3 (2009), pp. 294–316. DOI: https://doi.org/10.1016/j.nima.2009.01.001 (cited on pages 2, 3).

[5]   M. G. Aartsen et al. "Energy Reconstruction Methods in the IceCube Neutrino Telescope". In: *JINST* 9 (2014), P03009. DOI: 10.1088/1748-0221/9/03/P03009 (cited on page 3).

[6]   N. Kulacz. "In Situ Measurement of the IceCube DOM Efficiency Factor Using Atmospheric Minimum Ionizing Muons". MA thesis. University of Alberta, 2019 (cited on page 3).

[7]   R. Abbasi et al. "The design and performance of IceCube DeepCore". In: *Astropart. Phys.* 35.10 (2012), pp. 615–624. DOI: 10.1016/j.astropartphys.2012.01.004 (cited on page 3).

[8]   D. Chirkin and W. Rhode. "Propagating leptons through matter with Muon Monte Carlo (MMC)". In: (July 2004) (cited on page 5).

[9]   L. Raedel. "Simulation Studies of the Cherenkov Light Yield from Relativistic Particles in High-Energy Neutrino Telescopes with Geant4". MA thesis. Aachen, Germany: Rheinisch-Westfälischen Technischen Hochschule, 2012 (cited on pages 5, 7).

[10] P. A. Cherenkov. "Visible Radiation Produced by Electrons Moving in a Medium with Velocities Exceeding that of Light". In: *Phys. Rev.* 52 (4 Aug. 1937), pp. 378–379. DOI: 10.1103/PhysRev.52.378 (cited on page 5).

[11] S. Euler. "Observation of oscillations of atmospheric neutrinos with the IceCube Neutrino Observatory". PhD thesis. Aachen, Germany: Rheinisch-Westfälischen Technischen Hochschule, 2014 (cited on page 5).

[12] I. Frank and I. Tamm. "Coherent visible radiation from fast electrons passing through matter". In: *C. R. Acad. Sci. USSR* 14 (1937), pp. 109–114 (cited on page 5).

[13] L. Rädel and C. Wiebusch. "Calculation of the Cherenkov light yield from low energetic secondary particles accompanying high-energy muons in ice and water with Geant4 simulations". In: *Astroparticle Physics* 38 (Oct. 2012), pp. 53–67. DOI: 10.1016/j.astropartphys.2012.09.008 (cited on page 5).

[14] M. Tanabashi et al. "Review of Particle Physics". In: *Phys. Rev. D* 98 (3 Aug. 2018), p. 030001. DOI: 10.1103/PhysRevD.98.030001 (cited on page 6).

[15] J. P. Y. Garza. "Measurement of neutrino oscillations in atmospheric neutrinos with the IceCube DeepCore detector". PhD thesis. Berlin, Germany: Humboldt-Universität zu Berlin, Mathematisch-Naturwissenschaftliche Fakultät I, 2014. DOI: 10.18452/17016 (cited on page 9).

[16] J. Lundberg et al. "Light tracking for glaciers and oceans: Scattering and absorption in heterogeneous media with Photonics". In: *Nucl. Instrum. Meth.* A581 (2007), pp. 619–631. DOI: 10.1016/j.nima.2007.07.143 (cited on page 10).